

**NASA TECHNICAL  
MEMORANDUM**



**NASA TM X-52006**

**NASA TM X-52006**

**N 68-17288**

FACILITY FORM 602	(ACCESSION NUMBER)	(THRU)
	14	1
	(PAGES)	(CODE)
	TMX-52006	28
	(NASA CR OR TMX OR AD NUMBER)	(CATEGORY)

**THE OPERATION OF AN ELECTRON-BOMBARDMENT  
ION SOURCE WITH VARIOUS GASES**

by Paul D. Reader  
Lewis Research Center  
Cleveland, Ohio

TECHNICAL PREPRINT prepared for International  
Conference on Electron and Ion Beam Science and  
Technology sponsored by the Electrochemical  
Society and the American Institute of Mechanical  
Engineers

**GPO PRICE** \$ \_\_\_\_\_

**CFSTI PRICE(S)** \$ \_\_\_\_\_

Hard copy (HC) \_\_\_\_\_

Microfiche (MF) \_\_\_\_\_

ff 653 July 65

TECHNICAL MEMORANDUM

THE OPERATION OF AN ELECTRON-BOMBARDMENT  
ION SOURCE WITH VARIOUS GASES

by Paul D. Reader  
Lewis Research Center  
Cleveland, Ohio

TECHNICAL PREPRINT prepared for  
International Conference on Electron and Ion Beam Science  
and Technology sponsored by the Electrochemical Society  
and the American Institute of Mechanical Engineers ✓  
Toronto, Canada, May 5-7, 1964

NATIONAL AERONAUTICS AND SPACE ADMINISTRATION

N68-17288

X64-35461

## THE OPERATION OF AN ELECTRON-BOMBARDMENT

## ION SOURCE WITH VARIOUS GASES

by Paul D. Reader

NASA Lewis Research Center,  
Cleveland, Ohio

Code 2A

(NASA T M X 5757  
52006

## ABSTRACT

A

The efficiency of the electron-bombardment thruster is approaching the maximum that can be expected. Desired lifetimes (of the order of 10,000 hr) have not yet been reached, but present knowledge indicates such lifetimes should be obtainable. The simplicity of this thruster makes it interesting as an ion source for various laboratory experiments. Various gases have been used to determine the ion-chamber and accelerator performance for such applications.

[1964]

11 p ref  
990 4p

## INTRODUCTION

Several areas of work on the electron-bombardment thruster appear to be reaching completion. The ion-chamber configuration (ref. 1), magnetic field design (ref. 2), and the accelerator structure (ref. 3) all fall into this category. A possible exception might be an attempt to produce a more uniform current density, which would permit considerably greater average power densities for the same accelerator system lifetime.

The cathode is probably the most important component research area remaining for these thrusters. The cesium autocathode, with no apparent lifetime limit, is one promising solution. The use of cesium, however, places more severe limits on the thrust-to-area ratio at low specific impulse than does mercury. For this reason, continued research is warranted on cathodes employing alkaline-earth carbonates. Very substantial lifetimes (more than 1600 hr) have already been obtained with cathodes of this type in component tests.

The present efficiency of the electron-bombardment thruster ranges from about 60 percent at 4000 seconds specific impulse to about 80 percent at 10,000 seconds (ref. 4). These efficiencies are equivalent to power to thrust ratios of about 150 kilowatts per pound at 4000 seconds and almost 300 kilowatts per pound at 10,000 seconds. This performance is adequate for most proposed electric propulsion missions.

The simplicity and ruggedness of the electron-bombardment thruster also makes it interesting as an ion source for a variety of experiments. Plain tantalum or tungsten cathodes may be adequate for this application. Such cathodes have been evaluated for electric propulsion (ref. 5), and

Available to NASA Offices and  
NASA Centers Only.

X-52006

Crc

were found to be much less efficient and shorter-lived than the autocathode or oxide-matrix types, but the demonstrated lifetime of over 1000 hours should be sufficient for ion source applications. Also the ease of fabrication and operation make such cathodes a natural selection for this purpose.

Some plasma experiments in which the ion source is used simply to produce a beam or plasma column can use cesium or mercury, the elements of interest for propulsion. Other experiments, though, require the ionization of a number of elements. The performance of the ion-chamber and accelerator system were, therefore, evaluated with a number of gases - such as krypton, argon, nitrogen, helium, and hydrogen. This study was made with an existing 10-centimeter thruster that had been thoroughly investigated with mercury as the propellant. The data from these tests indicate the types of ions that this source can effectively produce.

#### APPARATUS AND PROCEDURE

A cutaway sketch of the 10-centimeter-diameter ion source used in these tests is shown in figure 1. The gas flow to the source is controlled by a calibrated leak. The material to be ionized passes through a flow distributor into the ionization chamber, which contains the cylindrical anode and an axially mounted cathode. An axial magnetic field prevents electrons, which are emitted from the cathode, from rapidly escaping to the anode. Escape of electrons to either end of the chamber is prevented by operating these ends at the same potential as the cathode. Some of the neutrals are ionized by the bombarding electrons, and some of these ions reach the perforated grid system at the downstream end of the chamber. This grid system (ion extraction system) focuses and accelerates the ions that reach the plane of the first grid into an ion exhaust beam. For thruster applications, a neutralizer (not shown in fig. 1) then current and charge neutralizes the ion beam.

The current density range at which ion chamber losses are minimized and accelerator durability is at an acceptable level occurs (for a 10-centimeter-diameter mercury source) for neutral flow rates equivalent to about 0.15 to 0.2 amperes of singly charged ions. The product of the equivalent neutral current, ionization cross-section, and the square root of molecular weight (which determines residence time for a fixed neutral temperature) was used (with mercury as the standard) as a scaling parameter to estimate a scaled flow rate for each gas tested. A constant value of this scaling relation implies a constant probability of ionization per unit path length of an ionizing electron. Flow rates above and below the values estimated from this simple scaling relation were explored to account for uncertainties in the relative values of ionization cross section and other discharge effects not included in the flow estimate.

Previous investigations have indicated that (with an optimized ion chamber geometry) the mechanism controlling the maximum propellant utiliza-

**Available to NASA Offices and  
NASA Centers Only.**

tion efficiency that can be obtained is probably the rapid escape of neutral atoms from the ionization chamber. It was anticipated, therefore, that the lighter gases, in a chamber optimized for mercury, would yield propellant utilization efficiencies lower than mercury.

The use of a 10-centimeter-diameter mercury ion thruster results in another limit that must be mentioned. The refractory metal cathode configuration used in this investigation burns out very rapidly at emission currents much above 10 amperes. This current restriction naturally limits the discharge power that can be obtained at a given discharge potential. This particular limit is noted in the discussion when it affects the data.

### DISCUSSION OF RESULTS

The usual method of comparing the performance of several electron-bombardment ion sources is to determine the discharge energy required to produce a beam ion. This energy, in electron volts per ion (ev/ion), is arrived at in the following manner:

$$\text{energy dissipated in} \\ \text{discharge per beam ion} = \frac{\text{discharge potential} \left( \frac{\text{discharge current} - \text{beam current}}{\text{beam current}} \right)}$$

Subtracting the beam current from the discharge (anode) current accounts for the low energy secondary electrons liberated in the ionization process. In the following discussion the discharge power dissipated per beam ion will be used to compare the ionization efficiencies obtained for each gas with that of mercury. All of the tests were performed with the same source except for certain modifications made for light gases - which will be described with the appropriate experimental data.

The curves of figure 2 are data obtained with the 10-centimeter-diameter ion source and presented in reference 6. The curves are intended to illustrate general trends rather than the absolute performance of the source.

Figure 2(a) shows the variation of energy dissipated in the discharge per beam ion with increasing mass utilization efficiency. As the utilization efficiency is increased, the energy required to ionize an additional amount of material increases and is asymptotic to 100 percent efficiency. The mass utilization efficiency is determined for mercury by dividing the beam current by the equivalent current of neutrals and operating the source at discharge potentials that minimize the percentage of multiply-charged ions (ref. 7). The values for the other source parameters, which were held constant except where noted, are presented on the figure.



The effect of increasing magnetic field on discharge losses is displayed in figure 2(b). As the containment of high-velocity ionizing electrons increases with increasing magnetic field, the losses at first drop rapidly, but then approach a constant value at a magnetic field strength that yields an electron cyclotron radius of about one-fifth the source radius.

Figure 2(c) shows the effect of discharge potential on ion chamber losses. At low potentials the ionization cross-section decreases rapidly and leads to large discharge currents to maintain a constant mass utilization efficiency. As the ion chamber potential difference (discharge potential) is increased, the losses go through a minimum. Above a discharge potential of about 50 volts, the percentage of multiply charged mercury ions becomes significant (ref. 7) and the initial assumption of singly ionized exhaust beam particles less accurate. The range of discharge potentials anticipated for propulsion applications are at the minimum discharge loss point or below because of cathode durability considerations (ref. 5).

The final curve (fig. 2(d)) indicates the effect of net accelerating potential on the energy dissipated in the ion chamber per beam ion. As the extraction field increases with a given geometry, the ions are withdrawn from the discharge more efficiently thus reducing the discharge losses per ion.

The first gas tested, krypton, gave excellent performance over a wide range of ion source operating conditions. The variation of source output with electrical parameters was qualitatively similar to operation with mercury. The general trends obtained with krypton are shown in figure 3. Figure 3(a) displays the trend of discharge losses with increasing mass utilization efficiency for several neutral flow rates. The flow rates that gave the best performance (low discharge power) were found to be equivalent to 0.35 to 0.5 amperes of singly ionized atoms. This range proved to be slightly lower than the 0.56 amperes estimated from the flow scaling relation mentioned previously. Mass utilization efficiencies up to 70 percent were obtained with krypton.

Figure 3(b) demonstrates the effect of magnetic field on the energy dissipated in the discharge for two neutral flow rates. An equivalent neutral flow rate of 0.42 amperes with a mass utilization efficiency of 53-percent resulted in a sharp increase in discharge losses when the minimum-loss field strength was exceeded. This trend is characteristic of a chamber operating off-design for the particular material being ionized. Similar characteristics are obtained for mercury with unusual flow distributors or very short ion chambers. Increasing the equivalent neutral flow rate to 0.64 amperes yielded a curve (dashed line) similar to that shown in figure 2(b) for mercury.

Figures 3(c) and (d) display the discharge loss trends for krypton with ion chamber potential difference and net accelerating potential, re-

spectively. As mentioned previously, the qualitative trends are similar to those of mercury (figs. 2(c) and (d)).

Argon gave results that were qualitatively similar to krypton and, hence, mercury. The effects of the electrical parameters on source output were more pronounced in that the optimum values of these parameters required to maximize output were quite well defined.

Figure 4(a) shows the energy dissipated in the discharge as a function of mass utilization efficiency for two argon flow rates. The parameters held constant are again given on the figure. The lowest level of discharge loss at a given mass utilization efficiency was obtained at a neutral flow rate equivalent to 1.0 ampere. This flow rate had been estimated at 0.8 amperes from the flow scaling relation. The maximum mass utilization efficiency that was obtained with argon was 50 percent. This limit occurred very nearly at the cathode emission limit. A greater discharge power capability would probably allow a slightly higher mass utilization efficiency with this gas.

Figures 4(b), (c), and (d) show the trends of ion chamber losses with magnetic field strength, ion chamber potential difference, and net accelerating potential, respectively. The results are similar to those obtained with mercury (fig. 2) and krypton (fig. 3).

After the above data had been obtained, a modification was made to the source in an effort to eliminate the effects of the ion chamber power (filament emission) restriction. An annular ring was placed upstream of the ion extraction system to reduce the exhaust beam diameter from 10 to 5 centimeters. The neutral flow rate was also reduced to 25 percent of the former values to match the reduction of accelerator area. This modification allowed the maximum discharge power per unit beam area to be raised by a factor of four without changing the filament emission limitation. The internal ion chamber geometry was not altered. A slightly higher mass utilization efficiency (55 percent) could be attained using argon with this configuration.

Nitrogen was the first diatomic gas tested in the program. The effect of small variations in electrical parameters became of increasing importance with this gas.

The neutral flow rate estimated from the previously mentioned scaling relation was 2.2 amperes of monatomic nitrogen. This flow rate was used as a starting point even though the annular plate had been used to reduce the flow area. (The annular plate was used for the balance of the program with lighter gases.)

Figure 5(a) shows the effect of mass utilization efficiency on ion chamber discharge losses for two values of neutral flow. The lowest discharge losses for a given mass utilization occur at flow rates correspond-

ing to about 3.0 amperes of atomic nitrogen ions. The mass utilization was calculated assuming that the exhaust beam was composed of singly charged atomic nitrogen ions ( $N^+$ ). The possible error in this assumption is indicated by measurements made by Nelson L. Milder at the Lewis Research Center with a quadrupole mass spectrometer utilizing a 5-centimeter-diameter electron-bombardment ion source. These measurements indicate that, between discharge potentials of 50 and 90 volts, 80 percent of the exhaust beam is composed of atomic nitrogen ions. The 10-centimeter-diameter ion source has also been shown to be an extremely effective molecular fragmentation device (ref. 8). However, no special effort was made to determine the percentages of  $N^+$  or  $N_2^+$  in the exhaust beam during this investigation. The best mass utilization efficiency obtained, assuming all  $N^+$ , was 23 percent (not shown on the figure). The actual mass utilization is probably slightly above this value due to the presence of some  $N_2^+$  ions.

Figure 5(b) shows the marked effect of magnetic field strength on the operation (discharge losses) of the source. Above 32 gauss and below 15 gauss, the discharge was extinguished. Figure 5(c) shows the general trend of discharge loss that has been typical of all types of ions with increasing extraction potential.

The operation of the source on both helium and hydrogen was very critical with regard to values of electrical parameters. Beam currents of about 0.35 amperes were obtained with both helium and hydrogen but at flow rates of about 25 and 31 amperes, respectively. The mass utilization efficiencies for both gases were, therefore, below 2 percent. The maximum mass utilization was severely hampered in both cases by the emission limit of the cathode. Accelerator impingement currents recorded throughout the program were consistently between 1 and 2 percent of the ion-beam current for every gas tested.

#### CONCLUDING REMARKS

The electron-bombardment thruster offers a simple and reliable ion source for a variety of experiments. The accelerating potential can be varied to provide a wide range of particle exhaust velocities, and the characteristics of the source allow it to be optimized for ionization of various gases.

The present study indicated that gases with atomic weights greater than that of argon can be ionized in a conventional ion source at mass utilization efficiencies of at least 50 percent. The reduction of mass utilization and the increasingly critical dependence of source operation on small ranges of electrical parameters with decreasing atomic weights are typical of nonoptimum source operation. Effects of this nature occur with the conventional mercury source either when it is operated at too low a propellant flow or when the chamber geometry is altered significantly from the optimum. It is anticipated that the mass utilization of any of the gases



tested could be improved by careful attention to flow and geometric configurations. Even without optimizing the source for a given gas, the utilization can be improved if larger cathode emission currents are possible. Larger discharge power requirements might demand a thruster cooling system, but this would not be a serious problem with a laboratory experiment.

#### REFERENCES

1. Reader, P. D.: Investigation of a 10-Centimeter-Diameter Electron-Bombardment Ion Rocket. NASA TN D-1163, 1962.
2. Reader, P. D.: An Electron-Bombardment Ion Rocket with a Permanent Magnet. AIAA Paper 63031, 1963. (See also Astronautics and Aerospace Eng., vol. 1, no. 9, Oct. 1963, p. 83.)
3. Kerslake, W. R.: Charge-Exchange Effects on the Accelerator Impingement of an Electron-Bombardment Ion Rocket. NASA TN D-1657, 1963.
4. Mickelsen, W. R., and Kaufman, H. R.: Status of Electrostatic Thrusters for Space Propulsion. NASA TN D-2172, 1964.
5. Milder, N. L., and Kerslake, W. R.: Evaluation of Filament Deterioration in Electron-Bombardment Ion Sources. NASA TN D-2173, 1964.
6. Reader, P. D.: Experimental Effect of Propellant Introduction Mode on Electron-Bombardment Ion Rocket Performance. Proposed NASA TN.
7. Milder, N. L.: Comparative Measurements of Singly and Doubly Ionized Mercury Produced by Electron-Bombardment Ion Engine. NASA TN D-1219, 1962.
8. Byers, D. C., Kerslake, W. R., and Grobman, J. S.: An Experimental Investigation of Heavy Molecule Propellants in an Electron-Bombardment Thruster. Proposed NASA TN.

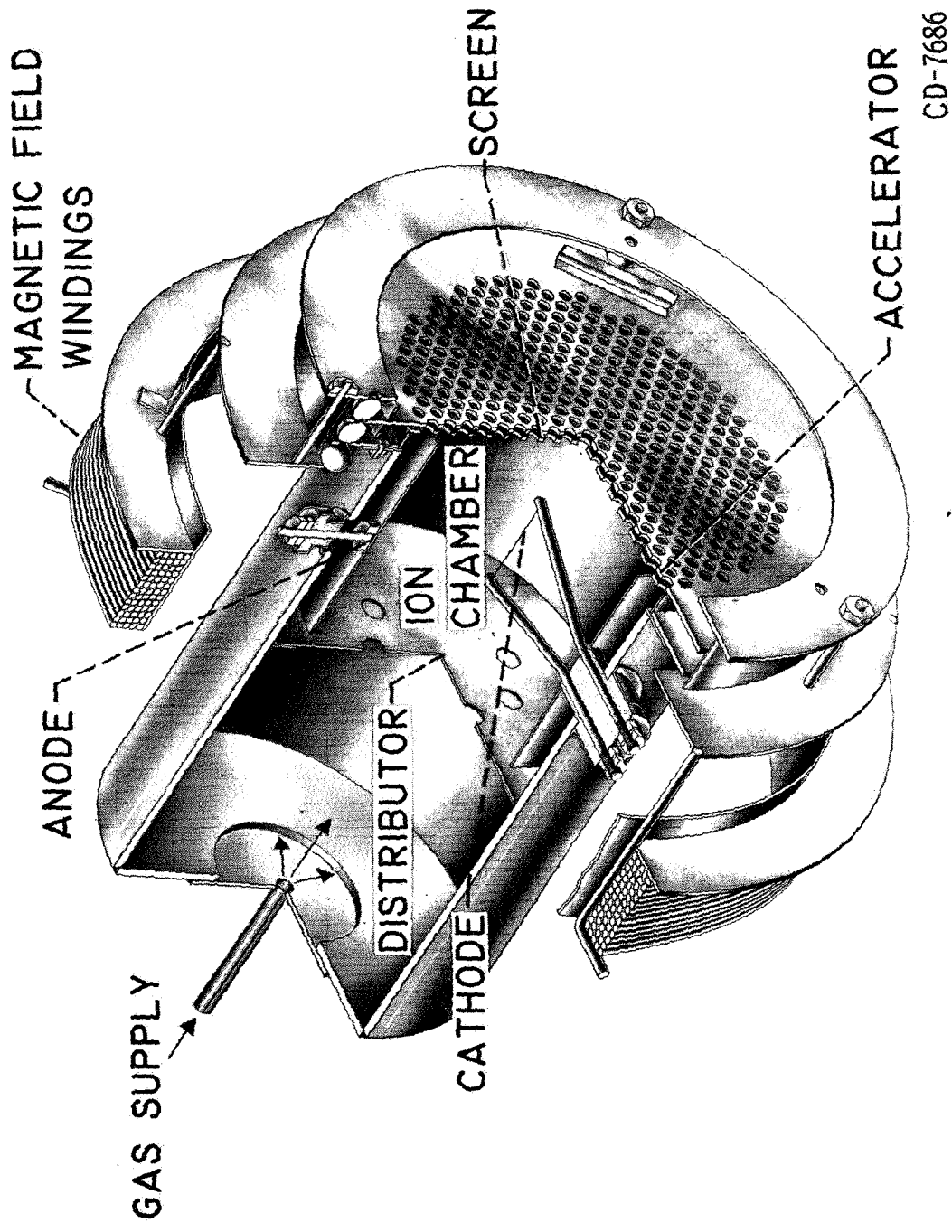
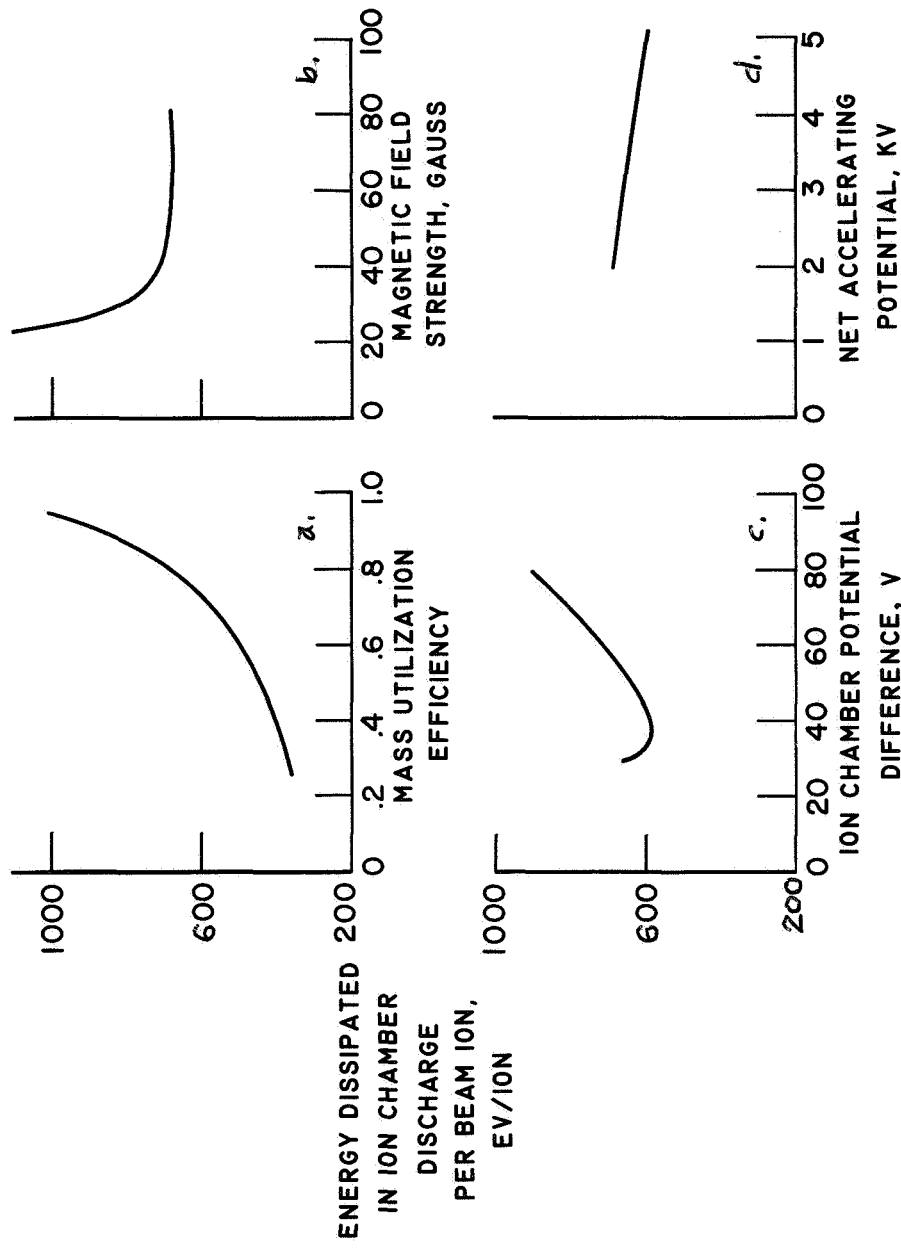


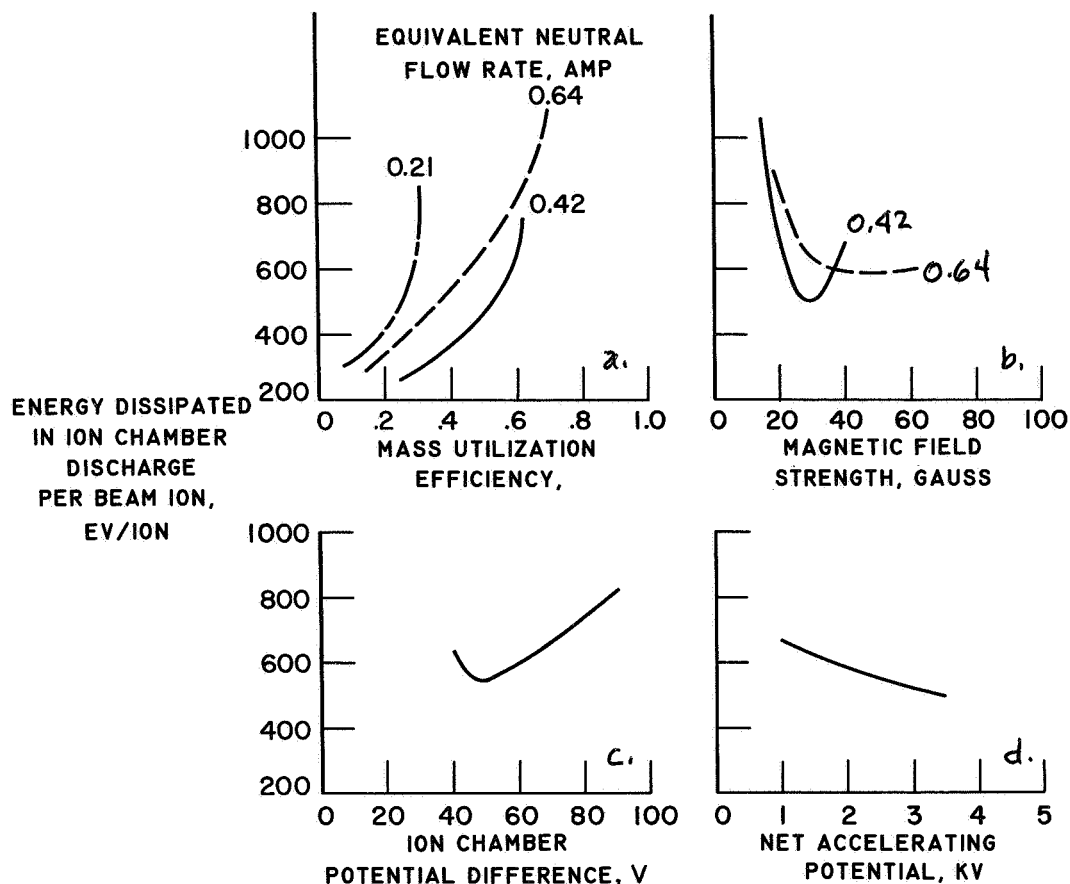
Figure 1. - 10-centimeter-diameter electron-bombardment ion source.



Parameters when not specified:

Mass utilization efficiency,	0.8	Net accelerating potential,	2.5 kv
Magnetic field strength,	40 gauss	Neutral flow rate,	0.16 amp
Ion chamber potential diff.,	50 v	Accelerator potential,	-2000 v

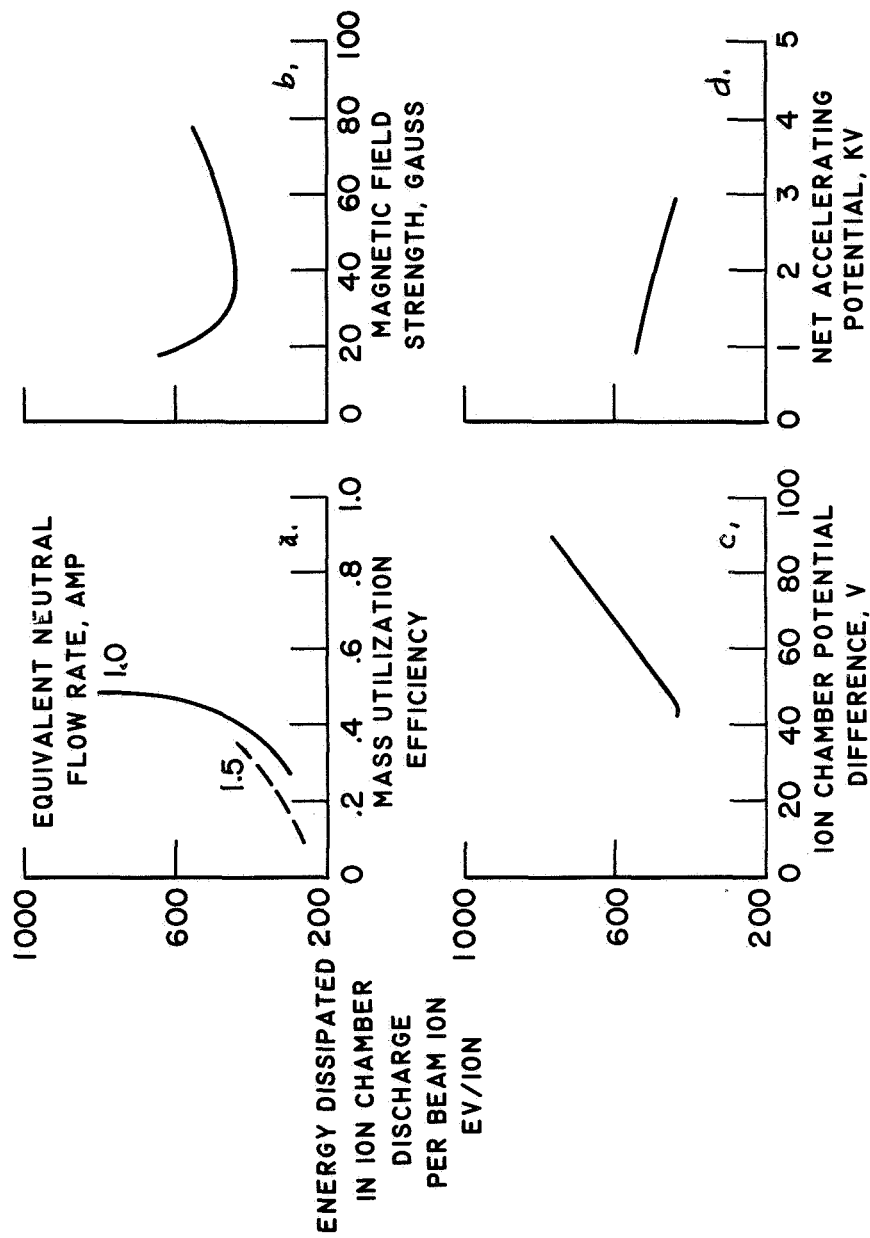
Figure 2. - Discharge performance of 10-centimeter-diameter electron-bombardment ion source using mercury.



Parameters when not specified:

Mass utilization efficiency,	0.53	Net accelerating potential,	2.5 kv
Magnetic field strength,	25 gauss	Neutral flow rate,	0.42 amp
Ion chamber potential diff.,	50 v	Accelerator potential,	-2000 v

Figure 3. - Discharge performance of 10-centimeter-diameter ion source using krypton.



Parameters when not specified:

Mass utilization efficiency,	0.4	Net accelerating potential,	2.5 kv
Magnetic field strength,	30 gauss	Neutral flow rate,	1.0 amp
Ion chamber potential diff.,	50 v	Accelerator potential,	-2000 v

Figure 4. - Discharge performance of 10-centimeter-diameter ion source using argon.